2018-04-28

Increased winter-mean wave height, variability and periodicity in the North-East Atlantic over 1949-2017

Masselink, Gerd

10.1002/2017gl076884
Geophysical Research Letters
American Geophysical Union

Increased winter-mean wave height, variability and periodicity in the North-East Atlantic over 1949-2017

Bruno Castelle[1,2], Guillaume Dodet[3], Gerd Masselink[4], Tim Scott[4]

Bruno Castelle, bruno.castelle@u-bordeaux.fr

[1]CNRS, UMR EPOC, France

[2]Univ. Bordeaux, UMR EPOC, France

[3]LETG-Brest Geomer UMR 6554 CNRS,

Institut Universitaire Europeen de la Mer

(UBO), Plouzane, France

[4]Coastal Processes Research Group,

School of Biological and Marine Sciences,

Plymouth University, UK

This article has been accepted for publication and undergone full peer review but has not been through the copyediting, typesetting, pagination and proofreading process, which may lead to differences between this version and the Version of Record. Please cite this article as doi: 10.1002/2017GL076884

A 69-year (1948-2017) numerical weather and wave hindcast is used to investigate the interannual variability and trend of winter wave height along the west coast of Europe. Results show that the winter-mean wave height, variability and periodicity all increased significantly in the northeast Atlantic over the last seven decades which primarily correlate with changes in the climate indices North Atlantic Oscillation (NAO) and West Europe Pressure Anomaly (WEPA) affecting atmospheric circulation in the North Atlantic. NAO and WEPA primarily explain the increase in winter-mean wave height and periodicity, respectively, while both WEPA and NAO explain the increase in interannual variability. This increase in trend, variability and periodicity resulted in more frequent high-energy winters with high NAO and/or WEPA over the last decades. The ability of climate models to predict the winter NAO and WEPA indices a few months ahead will be crucial to anticipate coastal hazards in this region.

Keypoints:

- Winter-mean wave height trend and variability along the entire west coast of Europe can be explained by the NAO and WEPA indices
- Winter-mean wave height, variability and periodicity all increased over the last seven decades
- Extreme winter-mean wave heights become more frequent as WEPA and NAO positivity and variability increase

1. Introduction

High-energy winter waves typically drive the largest amount of morphological variability from the nearshore zone [*Van Enckevort et al.*, 2004; *Ruessink et al.*, 2007; *Dubarbier et al.*, 2015] to the subaerial beach [e.g. *Ferreira*, 2005; *Masselink et al.*, 2016a; *Splinter et al.*, 2014; *Karunarathna et al.*, 2014] and up to the coastal dune [*Mull and Ruggiero*, 2014; *Castelle et al.*, 2015]. Severe beach and dune erosion can be caused by one severe storm or more commonly by the cumulative impact of a series of winter storms [*Barnard et al.*, 2011; *Splinter et al.*, 2014; *Karunarathna et al.*, 2014; *Masselink et al.*, 2016a]. Winter storm waves coinciding with high tides can also flood the hinterlands [*Chaumillon et al.*, 2017] and cause cliff failure [*Katz and Mushkin*, 2013; *Earlie et al.*, 2015] or transport boulder deposits inland [*Autret et al.*, 2016]. In addition, winter storm waves carry much more energy than during other seasons on most of the coastal regions worldwide, which could become an important renewable and sustainable energy resource [*Bromirski and Cayan*, 2015]. Large-scale changes in winter wave activity at the coast are therefore of critical importance for coastal scientists and engineers.

Winter wave activity is greatly influenced by large-scale patterns of atmospheric and oceanic variability on interannual and longer timescales. This variability can be explained by teleconnections at the global scale [e.g. *McPhaden et al.*, 2006], with climate oscillations showing varying degrees of periodicity. For instance the El Nino Southern Oscillation (ENSO) in the Pacific varies from 2-7 years, but the North Atlantic Oscillation (NAO) shows no significant perdiodicity [*Barbosa et al.*, 2006]. Winter wave energy in the Pacific Ocean is strongly affected by the ENSO and further modulated by the phase of other

climate indices such as the Pacific decadal oscillation [*Mantua et al.*, 1997]. The ENSO is therefore critical to winter wave energy across the Pacific [e.g. *Bromirski et al.*, 2013], with winter wave conditions in the northeast Pacific Ocean often opposite to those in the western and southern Pacific [*Barnard et al.*, 2015]. Extreme ENSO phases typically drive outstanding large-scale coastal erosion [*Barnard et al.*, 2017]. In addition to large-scale interannual variability patterns in winter wave height, an overall increase in winter wave energy has been captured since the 70s in many regions worldwide through both direct observation and modelled hindcasts [e.g. *Dodet et al.*, 2010; *Young et al.*, 2011]. Such an upward trend of the mean winter wave height combined with stable or even further increased decadal variability will inevitably result in increased coastal hazards and vulnerability.

The west coast of Europe, which comprises a wide range of low-lying and/or populated regions, is exposed to high-energy winter waves generated in the North Atlantic Ocean. The NAO is the dominant mode of atmospheric variability at mid-latitudes in the North Atlantic region [*Hurrell*, 1995], and it has therefore long been known that interannual to decadal variability of winter wave activity is strongly affected by the NAO [e.g. *Bacon and Carter*, 1993; *Dodet et al.*, 2010; *Izaguirre et al.*, 2010; *Martinez-Asensio et al.*, 2016]. However, the NAO primarily affects winter wave height variability in the northern latitudes, say north of 50°N. Recently, *Castelle et al.* [2017] developed a new climate index, namely the West Europe Pressure Anomaly (WEPA), which outscores all the conventional climate indices, including the NAO, in explaining winter wave height variability along the west coast of Europe, from the UK (52°N) to Portugal and even further south along the

northwest coast of Africa. The WEPA index is defined as the normalized sea level pressure (SLP) gradient between the stations Valentia (Ireland) and Santa Cruz de Tenerife (Canary Islands). The WEPA positive phase reflects an intensified and southward-shifted latitudinal SLP gradient across the east Atlantic, driving severe storms that funnel high-energy waves towards the west coast of Europe southwards of 52°N [*Castelle et al.*, 2017; *Malagon Santos et al.*, 2017]. This atmospheric pattern is not captured by the NAO. For instance the winter 2013/2014, which was characterized by a striking pattern of temporal and spatial extreme storm clustering [*Davies*, 2015] with the highest winter average wave height since at least 1948 [*Masselink et al.*, 2016b], was associated with an average positive NAO, but with the highest WEPA over the period. In addition to flooding issues in Western Europe [*Thorne*, 2014], these storms and associated storm waves caused dramatic coastal erosion and coastal structure damages [e.g. *Castelle et al.*, 2015; *Suanez et al.*, 2015; *Masselink et al.*, 2016a, b; *Pye and Blott*, 2016; *Autret et al.*, 2016].

Whether extreme winters such as that of 2013/2014 will repeat more frequently and/or will further intensify in the future is a key issue for the coastal regions of west Europe. It is therefore important to investigate if these extreme winters are already happening with increasing regularity and increased intensity. Wave buoy measurements, satellite altimeter measurements and numerical wave hindcasts all show a significant increase in winter wave height over the last decades in the northeast Atlantic, north of 50°N [e.g. *Bacon and Carter*, 1991, 1993; *Dodet et al.*, 2010; *Young et al.*, 2011; *Charles et al.*, 2012; *Bertin et al.*, 2013]. While trend magnitudes showed some variability between the studies, these trends have been shown to be much greater in the last half century than in the whole

last century and even beyond [*Wang et al.*, 2012]. In contrast, the change in interannual variability and periodicity of the winter wave activity has received much less attention. Addressing the trend and variability of the primary climate indices explaining winter activity in the northeast Atlantic (NAO and WEPA) provides a unique opportunity to extensively examine winter wave height temporal patterns along the west coast of Europe.

In this paper, we use a 69-year numerical weather and wave hindcast to address the trend, and interannual variability and periodicity of winter wave height along the Atlantic coast of Europe and their link to WEPA and NAO. It will be shown that the positive trend in winter wave height, primarily in the northern latitudes, together with the increased in periodicity, primarily in the southern latitudes, resulted in an increase in extreme winter-mean wave height along the west coast of Europe over the last decades. Whether or not this will carry on in the future as climate changes will have major implications from a coastal hazard perspective.

2. Data and methods

2.1. Wind-wave model hindcast

The same approach as detailed in *Masselink et al.* [2016b] and *Castelle et al.* [2017] was used to wind-wave model hindcast. In short, the 6-hourly SLP and 10-m wind fields $\vec{u}_{10}$ of the NCEP/NCAR reanalysis project [*Kalnay et al.*, 1996] were collected from January 1948 to April 2017. The wind field was further used to force the spectral wave model Wave Watch III V14.18 [*Tolman*, 2014] implemented on a 0.5° resolution grid covering the whole North Atlantic (80°-0°W; 0°-70°N). Although the wave modelling was extensively validated against wave buoys along the entire west coast of Europe in *Masselink et al.*

[2016b], the trends found with our wave model hindcast were also compared with those measured by some of the wave buoys and obtained through other reanalysese, namely ERA-Interim [1979-2017 *Dee et al.*, 2011] and ERA-20C [1900-2010 *Poli et al.*, 2016], which both do not include the period 2010-2017. Following the strategy developed in *Castelle et al.* [2017], six virtual wave buoys were used to address the spatial distribution of wave heights along the entire Atlantic coast of Europe from Scotland in the north to Portugal in the south (Figure 1b): SC: Scotland; IR: Ireland; BR: Brittany; BI: Biscay; GA: Galicia; PT: Portugal. Consistent with earlier studies [e.g. *Ouzeau et al.*, 2011; *Camus et al.*, 2014; *Martinez-Asensio et al.*, 2016; *Castelle et al.*, 2017], winter was defined as the period from December to March (DJFM). Winter averages of significant wave height Hs and its 95%, 98% and 99.5% exceedance values ($Hs_{95\%}$, $Hs_{98\%}$, $Hs_{99.5\%}$) were computed, resulting in 69 winters analyzed in this study, from the winter of 1948/1949 to that of 2016/2017. At each grid point, the normalized winter-mean significant wave height $\tilde{Hs}$ was further computed to allow an objective comparison of winter wave height variability in the different coastal regions of west Europe.

2.2. Climate indices

As detailed in *Castelle et al.* [2017], the winter WEPA was computed as the DJFM SLP difference anomaly between the stations Valentia (Ireland) and Santa Cruz de Tenerife (Canary Islands), see Fig. 1a. The SLP difference was further normalized over the same 69 winters as for the winter Hs. Well-known climate indices such as the NAO can be computed through the principal empirical orthogonal function (EOF) of surface pressure derived from a numerical weather hindcast to give a physically-based expression of

atmospheric structure [*Rogers*, 1981]. Instead, here we used the SLP difference definition of the NAO to be consistent with the WEPA time series, given that it is well established that the EOF- and SLP-based NAO indices show a very good agreement [*Hurrell and Deser*, 2009]. We used the DJFM SLP difference between the stations Reykjavik (Iceland) and Lisbon (Portugal) reflecting the variability between the Azores high and the Icelandic low [*Hurrell*, 1995, see Fig. 1a]. The SLP difference was further normalized over the 69 studied winters. At this stage it is important to note that NAO and WEPA are uncorrelated (correlation coefficient R of 0.02).

2.3. Wavelet analysis

We used the continuous wavelet transforms $W_n^z(s)$ on the climate indices and normalized winter Hs, defined as the convolution of a discrete sequence z_n ($n = 0,...,N\text{-}1$) with a scaled and normalized mother wavelet function ψ_0 (here Morlet):

$$W_n^z(s) = \left(\frac{\mathrm{dz}}{s}\right)^{1/2} \sum_{n'=0}^{N-1} z_{n'} \psi_0^* \left(\frac{(n'-n)\mathrm{dz}}{s}\right) \quad (1)$$

where dz is the uniform time step in z_n, n is time, s is the timescale [*Torrence and Compo*, 1998] and * is the complex conjugate. We also used the normalized bivariate extension of the continuous wavelet transform for two discrete sequences z_n and y_n of the same size, namely the wavelet-squared coherency $R_n^2(s)$ [*Jevrejeva et al.*, 2003; *Grinsted et al.*, 2004]:

$$R_n^2(s) = \frac{|S(s^{-1}W_n^{zy}(s))|^2}{S(s^{-1}W_n^z(s)).S(s^{-1}W_n^y(s))} \quad (2)$$

where S is a smoothing operator detailed in *Torrence and Webster* [1999] and *Grinsted et al.* [2004]. The wavelet analysis was performed on both the climate indices and $\tilde{H}s$ at the 6 virtual buoys. $W_n^z(s)$ was used to detect the dominant temporal modes of variability and how these modes vary in time, while $R_n^2(s)$ was used to measure the linear relationship, at a given timescale, between a climate index and a wave height time series as a function of time. A wavelet squared-coherency of 1 gives a perfect linear relationship between the two time series at a specific timescale at a given time, whereas a null value reflects the absence of linear correlation.

3. Results

Fig. 1 shows the spatial distribution of the correlation R between the winter-mean Hs and NAO (Fig. 1c) and WEPA (Fig. 1d). Consistent with earlier studies [e.g. *Dodet et al.*, 2010; *Shimura et al.*, 2013; *Bromirski and Cayan*, 2015; *Castelle et al.*, 2017], winter wave height variability at the northern latitudes is strongly correlated with NAO, where the winter-mean Hs is the largest (Fig. 1b). This relationship dramatically drops south of 52°N, that is, south of the Irish coast, to further weakly increase south of 40°N as winter-mean Hs and NAO become negatively correlated. In contrast, the WEPA index shows high correlation at the southern latitudes, with systematically $R > 0.8$ along the French, Spanish and Portuguese coasts (Fig. 1d). NAO and WEPA are therefore the two primary climate indices explaining winter wave height variability along the west coast of Europe, with WEPA giving the highest correlation from the south coast of Ireland and south west UK down to Morocco.

Fig. 2 provides insight into the time evolution of the NAO and WEPA indices as well as of the normalized winter wave height $\tilde{H}s$ at the six virtual buoys. A remarkable feature of the NAO is its trend toward a more positive phase over the last decades (positive trend of +13.0x10^{-3} per year, see dashed line in Fig. 2a). The NAO also shows some low-frequency variations although no preferred mode of variability can be depicted (Fig. 2b). In contrast, WEPA shows a much slower positive long-term trend (+4.6x10^{-3}, Fig. 2c) but shows large interannual variability with increased periodicity during the last three decades at a timescale of approximately 7 years (Fig. 2d). The winter wave variability at the 6 buoys is strongly affected by the trend and variability in NAO and WEPA. The long-term trend in normalized winter wave height increases from south to north (left-hand wave panels in Fig. 2) as the winter Hs increasingly correlates to the NAO. The two northern (SC, IR) and four southern (BR, BI, GA, PT) buoys best correlate with NAO (R is 0.80 - 0.92) and WEPA (R is 0.80 - 0.91), respectively. An important pattern is the systematic high wavelet power at the 7-year timescale since 1990 for the buoys BR, BI, GA and PT, and to a lesser extent the Irish buoy IR, together with a systematic high statistically significant coherency-squared values with WEPA at these timescales (see the four bottom panels of the right-hand column in Fig. 2). This shows that the atmospheric circulation changes explained by WEPA in the NE Atlantic have a profound influence on winter wave height variability and periodicity along the west coast of Europe south of 52°N, including a striking recent 7-year periodicity.

The overall recent increase in high wavelet power at most of the virtual buoys reveals an increase in winter wave height interannual variability which, together with an increase

in the mean, results in more extreme winters. Fig. 3 shows the spatial map of linear trend in winter-mean Hs (Fig. 3a), winter-mean $Hs_{98\%}$ (Fig. 3b) and of winter-mean Hs interannual variability (Fig. 3c). For the latter the time evolution of the 10-year moving standard deviation of local winter averaged Hs was linearly regressed. The choice of this 10-year period was motivated by the presence of most of local wavelet energy on the timescales shorter than 10 years (see second column of Fig. 2). Results show a large increase in winter average Hs over the last 69 years exceeding 10 mm/year offshore of Scotland and Ireland, i.e. an increase by more than 0.7 m over the study period. The rate of increase in winter average Hs decreases southwards to approximately 5 mm/year and 1 mm/year along the French and Portuguese coasts, respectively, although the trend is not statistically significant at the 95% level along the Spanish and Portuguese coasts. These patterns are essentially similar for the extreme wave heights $Hs_{95\%}$, $Hs_{98\%}$ and $Hs_{99.5\%}$ although the rates of increase are larger and the coverage of statistically significant trends is reduced. For instance for $Hs_{98\%}$ (Fig. 3b), which corresponds to approximately 58 hours of data per DJFM season, the increase in $Hs_{98\%}$ peaks at 24.8 mm/year (21.1 mm/year and 27.7mm/year for $Hs_{95\%}$ and $Hs_{99.5\%}$, respectively) meaning that $Hs_{98\%}$ increased by more than 1.7 m in 69 years off the Irish coast. Of note, removing the outstanding 2013/2014 does not alter these rates off the Irish coast, but substantially decrease those further south. For instance, an although the trends are not statistically significant at the 95% level, the increase in $Hs_{98\%}$ decreases by approximately 25% in the Bay of Biscay when ignoring the 2013/2014 winter. The patterns of the linear trend in winter Hs interannual variability are substantially different. Although the maximum

increase is located along the Irish coast (+ 1.2-1.4 %/year), most of the west coast of Europe also shows a large increase (+ 0.6-1 %/year). This large increase along all the west coast of Europe is largely due to the increased range in normalized winter Hs since the early 90s (see the 6 bottom left-hand panels in Fig. 2). Interestingly, both NAO and WEPA show the same rate of increase in interannual variability of +0.5 %/year (not shown).

4. Discussion and conclusions

The increase in winter Hs across the northeast Atlantic Ocean during the second half of the 20th century has long been studied [e.g. *Bacon and Carter*, 1991; *Charles et al.*, 2012; *Bertin et al.*, 2013]. Results show a maximum increase offshore of Ireland and Scotland with a gradual decrease southwards, similar in patterns with the peak wave period trend peaking at 0.01 s/year (not shown). Of note, no significant shift or trend in wave direction was found, as the trend in winter-mean wave direction is systematically smaller than 0.05°/year and not statistically significant at the 95% level along the entire Atlantic coast of Europe (not shown). This result corroborates the findings of *Dodet* [2013] and means that this change in winter-mean wave height was not associated with a distinct shift in the wave generation location. A salient result is the clear increase in winter wave height interannual variability, which shows different patterns to those of the increase in the mean (Fig. 3c). Although peaking offshore of Ireland, the entire Atlantic coast of Europe has been exposed to an increase in winter wave interannual variability. While the most northern buoy (Scotland: SC) shows high and small correlation with NAO and WEPA, respectively, it is the opposite for the southern buoy of Galicia (GA). In fact the

west coast of Europe forms a continuum where winter wave height variability, from north to south, is decreasingly and increasingly correlated with NAO and WEPA, respectively. This is also reflected in the mean trend, with the northern buoys showing large increase in the mean over the last decades, consistent with the long-term trend of the NAO. In contrast, the southern buoys show a striking increase in periodicity of approximately 7 years over the last 3 decades, which is essentially controlled by the WEPA index.

The increase in the mean (primarily linked to NAO) together with the increased variability and periodicity (primarily linked to WEPA) resulted in more extreme positive climate index phases and, in turn, in more extreme winter waves. For instance, 11 out of the 12 largest NAO values are found in the second half of the time series from the 1988/1989 to the 2016/2017 winters (Fig. 2a). For WEPA, four out of the five largest WEPA (> 1.6) are found during the same period. This is further emphasized in Fig. 4 (see the largest circle size in the last 3 decades) which shows that, while the NAO and WEPA are clearly uncorrelated, the respective contribution of WEPA and NAO to winter Hs varies from north to south with winter Hs quasi-independent of WEPA and NAO at the northern and southern latitudes, respectively (left-hand panels in Fig. 4). It is clear that there has been an increased number of extreme winters along most of the coast with high values of either NAO and/or WEPA index.

Fig. 4 also provides physical insight into the atmospheric and wave height expression of the two winter with the highest Hurrell-definition NAO index (winter 1988/1989, Fig. 4b,c) and the winter with the highest WEPA index (winter 2013/2014, Fig. 4e,f), which are representative of recent extreme winter-mean Hs situations along the west coast of

Europe. During the winter 1988/1989 (NAO index of +2.19), the widening and strengthening of the anticyclone centered on the Azores and the lowering pressures in high latitudes resulted in increased W-SW winds around 60°N. This atmospheric pattern drove larger winter waves at northern latitudes (Irish and Scottish coast, Fig. 4b), with an increase with respect to the mean peaking at 1.60 m offshore of the Scottish coast (Fig. 4c). During the winter 2013/2014 (WEPA index of 2.66), the latitudinal atmospheric dipole of anomaly resembled the 15° southward-shifted 1988/1989 pattern together with a substantial longitudinal anomaly driving increased W-NW winds around 45°N funneling towards the west coast of Europe (Fig. 4e). This generated larger waves along the entire coast of Europe, down to northwest Africa, peaking at +1.62 m at approximately 50°N (Fig. 4f). This situation may become more common during the next decades if the trend in both winter-mean wave height trend and interannual variability continues. In contrast with the recent increased in extreme winter along most of the coast with high values of either NAO and/or WEPA index, fewer occurrences in the lower-left quadrant (WEPA and NAO both negative) are observed. These correspond to low winter wave height along most of the west coast Europe. This configuration is increasingly rare as more than half these winters were observed during the 20 first years of the 1949-2017 time series. For more information on storm track and atmospheric circulation changes related to NAO and WEPA, the reader is referred to *Castelle et al.* [2017].

Increasing winter wave height and interannual variability and periodicity is highlighted in this study, while the climate has already changed over the last decades. This suggests that this evolution could continue over the next decades, with more extreme winters as

described in the right-hand panels of Fig. 4. However, most of the existing climate models indicate that there will be no increase in winter Hs in the northeast Atlantic, or even a decrease as stated in *Hemer et al.* [2013], in the frame of climate change even for the worst-case emission scenario [e.g. *Wang et al.*, 2014; *Aarnes et al.*, 2017]. A notable exception is the study of *Zappa et al.* [2013] who showed a systematic increase in the number of European extratropical cyclones with increasing emission. In other words, the variability and trend described in this study go against most of the existing long-term wave model forecasts. It will therefore be critical to address the evolution of the winter wave height over the next years and decades to explore if the recent increase in the mean, variability and periodicity is related to a natural anomaly or if it is the expression of climate change.

Trend magnitudes computed from wind-wave model hindcasts must be used carefully as the progressive or abrupt assimilation of new field and satellite data is known to impact surface winds and, in turn, wave characteristics [*Sasaki*, 2016]. Although not shown here, comparison with other reanalyses indicate that, over the period 1980-2010, our wind-wave model hindcast gives very similar trends in both pattern and magnitude to the most recent ERA-20C, while ERA-Interim yields spurious trends in wave height, as already noted by *Aarnes et al.* [2015]. Running the same analysis over 1948-2010 shows that ERA-20C gives slightly smaller positive trends in winter-mean wave height, with for instance a decrease up to approximately 50% in trend offshore of the Irish coast. ERA-20C also shows a southward shift of the maximum increase in winter-mean wave height variability by approximately 5°. Comparison with winter-mean wave height measured at the wave buoys GA (WMO62001) and K1 (WMO62029) (Fig. 1a), which are the longest

wave records in this region, also show similar magnitude trends with our model hindcast. Our wave hindcast even slightly underestimates the increase in winter-mean wave height. However, the winter-mean wave height trends are not statistically significant at the 95% level owing to data gaps and the relatively short time series (¡20 years). It is now well established that winter-mean wave height variability is correlated with a combination of WEPA and NAO. Here, WEPA and NAO indices, which are computed with reliable in situ SLP measurements, consistently show this increase in the mean (primarily NAO) and in variability and periodicity (primarily WEPA). The authors therefore believe that this increase is reliable but that magnitude in winter-mean trend and the patterns of the increased variability can be further improved using more advanced wind-wave model hindcasts.

Winter wave height variability was addressed here because winter storm wave height is the primary parameter affecting dune erosion and cliff failure [e.g. *Earlie et al.*, 2015], and coastal hazards overall. In addition, wave height variability alone can explain 70-80% of shoreline variability along open sandy coasts [e.g. *Yates et al.*, 2009; *Castelle et al.*, 2014]. However, changes in winter-mean wave period and direction and/or local winds can also affect sediment transport pathways and resulting coastal hazards through for instance beach rotation in coastal embayments [e.g. *Harley et al.*, 2011]. Such investigation is site specific and requires the use of nested and high-resolution wave, flow and sediment transport and wind models, which is beyond the scope of this study.

Increasing winter wave height and interannual variability and periodicity along the Atlantic coast of Europe is controlled by changes in atmospheric circulation primarily

described through WEPA and NAO. Although chaotic and unpredictable variability still dominates in many cases, recent research has provided evidence of increased skill in seasonal seasonal predictability of the NAO using the latest generation forecasting systems [*Scaife et al.*, 2014; *Dunstone et al.*, 2016; *Scaife et al.*, 2017]. The seasonal predictability of WEPA using these latest forecast systems had not yet studied in detail. Given that the combination of NAO and WEPA allows the determination of winter-mean wave height along the entire west coast of Europe, the ability of the Climate models to predict the winter NAO and WEPA climate indices a few months ahead will be crucial to anticipate coastal hazards in this region of the world.

Acknowledgments. This work was financially supported by the *Agence Nationale de la Recherche* (ANR) through the project SONO (ANR-17-CE01-0014) and the "Laboratoire d'Excellence" LabexMER (ANR-10-LABX-19-01) program, and by the AST "Evenements extremes" of the *Observatoire Aquitain des Sciences de l'Univers* (OASU). GD was funded by the research program PROTEVS (12CR6) conducted by the French Naval Oceanographic and Hydrographic Department (SHOM). GM and TS were funded by the NERC BLUE-coast project (NE/N015525/1). We acknowledge the SLP data providers in the ECA&D project [http://www.ecad.eu, *Klein Tank et al.*, 2002] and the Irish Meteorological Service (http://www.met.ie/climate-request/) for the Valentia Observatory data, the developers of the WAVEWATCH III TM model, the NCEP Reanalysis data provided by the NOAA/OAR/ESRL PSD and the ECMWF ERA-Interim and ERA-40 dataset (www.ECMWF.Int/research/Era). The DJFM time series of WEPA, NAO and WW3 Hs that were used for the whole analysis are provided as supplementary material

of this paper. We thank the two anonymous reviewers for constructive comments and suggestions.

References

Aarnes, O. J., S. Abdalla, J.-R. Bidlot, and O. Breivik (2015), Marine wind and wave height trends at different era-interim forecast ranges, *Journal of Climate*, *28*(2), 819–837, doi:10.1175/JCLI-D-14-00470.1.

Aarnes, O. J., M. Reistad, O. Breivik, E. Bitner-Gregersen, L. Ingolf Eide, O. Gramstad, A. K. Magnusson, B. Natvig, and E. Vanem (2017), Projected changes in significant wave height toward the end of the 21st century: Northeast atlantic, *Journal of Geophysical Research: Oceans*, *122*(4), 3394–3403, doi:10.1002/2016JC012521.

Autret, R., G. Dodet, B. Fichaut, S. Suanez, L. David, F. Leckler, F. Ardhuin, J. Ammann, P. Grandjean, P. Lallemand, and J. F. Philipot (2016), A comprehensive hydro-geomorphic study of cliff-top storm deposits on Banneg Island during winter 2013-2014, *Marine Geology*, *382*, 37 – 55.

Bacon, S., and D. J. T. Carter (1991), Wave climate changes in the north atlantic and north sea, *International Journal of Climatology*, *11*(5), 545–558, doi:10.1002/joc.3370110507.

Bacon, S., and D. J. T. Carter (1993), A connection between mean wave height and atmospheric pressure gradient in the north atlantic, *International Journal of Climatology*, *13*(4), 423–436, doi:10.1002/joc.3370130406.

Barbosa, S., M. E. Silva, and M. J. Fernandes (2006), Wavelet analysis of the lisbon and gibraltar north atlantic oscillation winter indices, *International Journal of Climatology*,

26(5), 581–593, doi:10.1002/joc.1263.

Barnard, P., A. Short, M. Harley, K. Splinter, S. Vitousek, I. Turner, J. Allan, M. Banno, K. Bryan, A. Doria, J. Hansen, S. Kato, Y. Kuriyama, E. Randall-Goodwin, P. Ruggiero, I. Walker, and D. Heathfield (2015), Coastal vulnerability across the Pacific dominated by El Nino/Southern Oscillation, *Nature Geoscience*, *8*(10), 801–807, doi:10.1038/ngeo2539.

Barnard, P., D. Hoover, D. Hubbard, A. Snyder, B. Ludka, J. Allan, G. Kaminsky, P. Ruggiero, T. Gallien, L. Gabel, D. McCandless, H. Weiner, N. Cohn, D. Anderson, and K. Serafin (2017), Extreme oceanographic forcing and coastal response due to the 2015-2016 el nino, *Nature Communications*, *8*, doi:10.1038/ncomms14365.

Barnard, P. L., J. Allan, J. E. Hansen, G. M. Kaminsky, P. Ruggiero, and A. Doria (2011), The impact of the 2009-10 el nino modoki on u.s. west coast beaches, *Geophysical Research Letters*, *38*(13), doi:10.1029/2011GL047707, l13604.

Bertin, X., E. Prouteau, and C. Letetrel (2013), A significant increase in wave height in the North Atlantic Ocean over the 20th century, *Global and Planetary Change*, *106*, 77–83.

Bromirski, P. D., and D. R. Cayan (2015), Wave power variability and trends across the North Atlantic influenced by decadal climate patterns, *Journal of Geophysical Research: Oceans*, *120*(5), 3419–3443, doi:10.1002/2014JC010440.

Bromirski, P. D., D. R. Cayan, J. Helly, and P. Wittmann (2013), Wave power variability and trends across the north pacific, *Journal of Geophysical Research: Oceans*, *118*(12), 6329–6348, doi:10.1002/2013JC009189.

Camus, P., M. Menendez, F. J. Mendez, C. Izaguirre, A. Espejo, V. Canovas, J. Perez, A. Rueda, I. J. Losada, and R. Medina (2014), A weather-type statistical downscaling framework for ocean wave climate, *Journal of Geophysical Research: Oceans*, *119*(11), 7389–7405, doi:10.1002/2014JC010141.

Castelle, B., V. Marieu, S. Bujan, S. Ferreira, J. P. Parisot, S. Capo, N. Senechal, and T. Chouzenoux (2014), Equilibrium shoreline modelling of a high-energy meso-macrotidal multiple-barred beach, *Marine Geology*, *347*, 85–94.

Castelle, B., V. Marieu, S. Bujan, K. D. Splinter, A. Robinet, N. Senechal, and S. Ferreira (2015), Impact of the winter 2013-2014 series of severe Western Europe storms on a double-barred sandy coast: Beach and dune erosion and megacusp embayments, *Geomorphology*, *238*, 135–148.

Castelle, B., G. Dodet, G. Masselink, and T. Scott (2017), A new climate index controlling winter wave activity along the atlantic coast of europe: The west europe pressure anomaly, *Geophysical Research Letters*, *44*(3), 1384–1392, doi:10.1002/2016GL072379.

Charles, E., D. Idier, J. Thiebot, G. L. Cozannet, R. Pedreros, F. Ardhuin, and S. Planton (2012), Present wave climate in the bay of biscay: Spatiotemporal variability and trends from 1958 to 2001, *Journal of Climate*, *25*(6), 2020–2039, doi:10.1175/JCLI-D-11-00086.1.

Chaumillon, E., X. Bertin, A. Fortunato, M. Bajo, J.-L. Schneider, L. Dezileau, J. P. Walsh, A. Michelot, E. Chauveau, A. Creach, A. Henaff, T. Sauzeau, B. Waeles, B. Gervais, G. Jan, J. Baumann, J.-F. Breilh, and R. Pedreros (2017), Storm-induced marine flooding: Lessons from a multidisciplinary approach, *Earth-Science Reviews*, *165*, 151

– 184, doi:https://doi.org/10.1016/j.earscirev.2016.12.005.

Davies, H. C. (2015), Weather chains during the 2013/2014 winter and their significance for seasonal prediction, *Nature Geoscience*, *8*, 833–837.

Dee, D. P., S. M. Uppala, A. J. Simmons, P. Berrisford, P. Poli, S. Kobayashi, U. Andrae, M. A. Balmaseda, G. Balsamo, P. Bauer, P. Bechtold, A. C. M. Beljaars, L. van de Berg, J. Bidlot, N. Bormann, C. Delsol, R. Dragani, M. Fuentes, A. J. Geer, L. Haimberger, S. B. Healy, H. Hersbach, E. V. Holm, L. Isaksen, P. Kallberg, M. Kohler, M. Matricardi, A. P. McNally, B. M. Monge-Sanz, J.-J. Morcrette, B.-K. Park, C. Peubey, P. de Rosnay, C. Tavolato, J.-N. Thepaut, and F. Vitart (2011), The era-interim reanalysis: configuration and performance of the data assimilation system, *Quarterly Journal of the Royal Meteorological Society*, *137*(656), 553–597, doi:10.1002/qj.828.

Dodet, G. (2013), Morphodynamic modelling of a wave-dominated tidal inlet : the albufeira lagoon, Ph.D. thesis, Université de La Rochelle, 178 pages.

Dodet, G., X. Bertin, and R. Taborda (2010), Wave climate variability in the north-east atlantic ocean over the last six decades, *Ocean Modelling*, *31*(3-4), 120 – 131.

Dubarbier, B., B. Castelle, V. Marieu, and G. Ruessink (2015), Process-based modeling of cross-shore sandbar behavior, *Coastal Engineering*, *95*, 35 – 50, doi:http://dx.doi.org/10.1016/j.coastaleng.2014.09.004.

Dunstone, N., D. Smith, A. A. Scaife, L. Hermanson, R. Eade, N. Robinson, M. Andrew, and J. R. Knight (2016), Skilful predictions of the winter north atlantic oscillation one year ahead, *Nature Geoscience*, *9*, 809–814, doi:10.1038/ngeo2824.

Earlie, C. S., A. P. Young, G. Masselink, and P. E. Russell (2015), Coastal cliff ground motions and response to extreme storm waves, *Geophysical Research Letters*, *42*(3), 847–854, doi:10.1002/2014GL062534.

Ferreira, O. (2005), Storm groups versus extreme single storms: predicted erosion and management consequences, *Journal of Coastal Research*, *SI 42*, 221–227.

Grinsted, A., J. C. Moore, and S. Jevrejeva (2004), Application of the cross wavelet transform and wavelet coherence to geophysical time series, *Nonlinear Processes in Geophysics*, *11*, 561–566.

Harley, M. D., I. L. Turner, A. D. Short, and R. Ranasinghe (2011), A reevaluation of coastal embayment rotation: The dominance of cross-shore versus alongshore sediment transport processes, Collaroy-Narrabeen Beach, southeast Australia, *Journal of Geophysical Research*, *116*(F04033), doi:10.1029/2010JF001989.

Hemer, M., Y. Fan, N. Mori, A. Semedo, and X. Wang (2013), Projected changes in wave climate from a multi-model ensemble, *Nature Climate Change*, *3*(5), 471–476, doi:10.1038/nclimate1791.

Hurrell, J. W. (1995), Decadal Trends in the North Atlantic Oscillation: Regional Temperatures and Precipitation, *Science*, *269*(5224), 676–679, doi: 10.1126/science.269.5224.676.

Hurrell, J. W., and C. Deser (2009), North Atlantic climate variability: The role of the North Atlantic Oscillation , *Journal of Marine Systems*, *78*(1), 28 – 41.

Izaguirre, C., F. J. Mendez, M. Menedez, A. Luceno, and I. J. Losada (2010), Extreme wave climate variability in Southern Europe using satellite data, *Journal of Geophysical*

Research, *C04009*, doi::10.1029/2009JC005802.

Jevrejeva, S., J. C. Moore, and A. Grinsted (2003), Influence of the Arctic Oscillation and El Niño-Southern Oscillation (ENSO) on ice conditions in the Baltic sea: The wavelet approach, *Journal of Geophysical Research*, *108*(D21), doi:10.1029/2003JD003417.

Kalnay, E., M. Kanamitsu, R. Kistler, W. Collins, D. Deaven, L. Gandin, M. Iredell, S. Saha, G. White, J. Woollen, Y. Zhu, A. Leetmaa, R. Reynolds, M. Chelliah, W. Ebisuzaki, W. Higgins, J. Janowiak, K. C. Mo, C. Ropelewski, J. Wang, R. Jenne, and D. Joseph (1996), The NCEP/NCAR 40-Year Reanalysis Project, *Bulletin of the American Meteorological Society*, *77*(3), 437–471.

Karunarathna, H., D. Pender, R. Ranasinghe, A. D. Short, and D. E. Reeve (2014), The effect of storm clustering on beach profile variability, *Marine Geology*, *348*, 103–112.

Katz, O., and A. Mushkin (2013), Characteristics of sea-cliff erosion induced by a strong winter storm in the eastern mediterranean, *Quaternary Research*, *80*(1), 20 – 32, doi: http://dx.doi.org/10.1016/j.yqres.2013.04.004.

Klein Tank, A. M. G., J. B. Wijngaard, G. P. Konnen, R. Bohm, G. Demaree, A. Gocheva, M. Mileta, S. Pashiardis, L. Hejkrlik, C. Kern-Hansen, R. Heino, P. Bessemoulin, G. Muller-Westermeier, M. Tzanakou, S. Szalai, T. Palsdottir, D. Fitzgerald, S. Rubin, M. Capaldo, M. Maugeri, A. Leitass, A. Bukantis, R. Aberfeld, A. F. V. van Engelen, E. Forland, M. Mietus, F. Coelho, C. Mares, V. Razuvaev, E. Nieplova, T. Cegnar, J. Antonio Lopez, B. Dahlstrom, A. Moberg, W. Kirchhofer, A. Ceylan, O. Pachaliuk, L. V. Alexander, and P. Petrovic (2002), Daily dataset of 20th-century surface air temperature and precipitation series for the European Climate Assessment, *International*

Journal of Climatology, *22*(12), 1441–1453, doi:10.1002/joc.773.

Malagon Santos, V., I. D. Haigh, and W. Thomas (2017), Spatial and temporal clustering analysis of extreme wave events around the uk coastline, *Journal of Marine Science and Engineering*, *5*(3), doi:10.3390/jmse5030028.

Mantua, N. J., S. R. Hare, Y. Zhang, J. M. Wallace, and R. C. Francis (1997), A pacific interdecadal climate oscillation with impacts on salmon production, *Bulletin of the American Meteorological Society*, *78*(6), 1069–1079, doi:10.1175/1520-0477(1997)078¡1069:APICOW¿2.0.CO;2.

Martinez-Asensio, A., M. N. Tsimplis, M. Marcos, X. Feng, D. Gomis, G. Jorda, and S. A. Josey (2016), Response of the North Atlantic wave climate to atmospheric modes of variability, *International Journal of Climatology*, *36*(3), 1210–1225, doi:10.1002/joc.4415.

Masselink, G., T. Scott, T. Poate, P. Russell, M. Davidson, and D. Conley (2016a), The extreme 2013/2014 winter storms: hydrodynamic forcing and coastal response along the southwest coast of England, *Earth Surface Processes and Landforms*, *41*(3), 378–391, doi:10.1002/esp.3836.

Masselink, G., B. Castelle, T. Scott, G. Dodet, S. Suanez, D. Jackson, and F. Floc'h (2016b), Extreme wave activity during 2013/2014 winter and morphological impacts along the Atlantic coast of Europe, *Geophysical Research Letters*, *43*(5), 2135–2143, doi:10.1002/2015GL067492.

McPhaden, M. J., S. E. Zebiak, and M. H. Glantz (2006), ENSO as an Integrating Concept in Earth Science, *Science*, *314*(5806), 1740–1745, doi:10.1126/science.1132588.

Mull, J., and P. Ruggiero (2014), Estimating storm-induced dune erosion and overtopping along u.s. west coast beaches, *Journal of Coastal Research*, pp. 1173–1187, doi: 10.2112/JCOASTRES-D-13-00178.1.

Ouzeau, G., J. Cattiaux, H. Douville, A. Ribes, and D. Saint-Martin (2011), European cold winter 2009-2010: How unusual in the instrumental record and how reproducible in the arpege-climat model?, *Geophysical Research Letters*, *38*(11), doi: 10.1029/2011GL047667, l11706.

Poli, P., H. Hersbach, D. P. Dee, P. Berrisford, A. J. Simmons, F. Vitart, P. Laloyaux, D. G. H. Tan, C. Peubey, J.-N. Thepaut, Y. Tremolet, E. V. Holm, M. Bonavita, L. Isaksen, and M. Fisher (2016), Era-20c: An atmospheric reanalysis of the twentieth century, *Journal of Climate*, *29*(11), 4083–4097, doi:10.1175/JCLI-D-15-0556.1.

Pye, K., and S. J. Blott (2016), Assessment of beach and dune erosion and accretion using LiDAR: Impact of the stormy 2013-14 winter and longer term trends on the Sefton Coast, UK, *Geomorphology*, *266*, 146 – 167, doi: http://dx.doi.org/10.1016/j.geomorph.2016.05.011.

Rogers, J. C. (1981), Spatial Variability of Seasonal Sea Level Pressure and 500 mb Height Anomalies, *Monthly Weather Review*, *109*(10), 2093–2106.

Ruessink, B. G., Y. Kuriyama, A. J. H. M. Reniers, and J. A. Roelvink (2007), Modeling cross-shore sandbar behavior on the timescales of weeks, *Journal of Geophysisical Research*, *112*(F03010), doi:10.1029/2006JC000730.

Sasaki, W. (2016), Impact of satellite data assimilation in atmospheric reanalysis on the marine wind and wave climate, *Journal of Climate*, *29*(17), 6351–6361, doi:

10.1175/JCLI-D-16-0056.1.

Scaife, A. A., A. Arribas, E. Blockley, A. Brookshaw, R. T. Clark, N. Dunstone, R. Eade, D. Fereday, C. K. Folland, M. Gordon, L. Hermanson, J. R. Knight, D. J. Lea, C. MacLachlan, A. Maidens, M. Martin, A. K. Peterson, D. Smith, M. Vellinga, E. Wallace, J. Waters, and A. Williams (2014), Skillful long-range prediction of european and north american winters, *Geophysical Research Letters*, *41*(7), 2514–2519, doi:10.1002/2014GL059637, 2014GL059637.

Scaife, A. A., R. Comer, N. Dunstone, D. Fereday, C. Folland, E. Good, M. Gordon, L. Hermanson, S. Ineson, A. Karpechko, J. Knight, C. MacLachlan, A. Maidens, K. A. Peterson, D. Smith, J. Slingo, and B. Walker (2017), Predictability of european winter 2015/2016, *Atmospheric Science Letters*, *18*(2), 38–44, doi:10.1002/asl.721.

Shimura, T., N. Mori, and H. Mase (2013), Ocean Waves and Teleconnection Patterns in the Northern Hemisphere, *Journal of Climate*, *26*(21), 8654–8670, doi:10.1175/JCLI-D-12-00397.1.

Splinter, K. D., J. T. Carley, A. Golshani, and R. Tomlinson (2014), A relationship to describe the cumulative impact of storm clusters on beach erosion, *Coastal Engineering*, *83*, 49–55.

Suanez, S., R. Cancouet, F. Floc'h, E. Blaise, F. Ardhuin, J.-F. Filipot, J.-M. Cariolet, and C. Delacourt (2015), Observations and predictions of wave runup, extreme water levels, and medium-term dune erosion during storm conditions, *Journal of Marine Science and Engineering*, *3*(3), 674, doi:10.3390/jmse3030674.

Thorne, C. (2014), Geographies of uk flooding in 2013/4, *The Geographical Journal*, *180*(4), 297–309, doi:10.1111/geoj.12122.

Tolman, H. L. (2014), User manual and system documentation of WAVEWATCH III version 4.18, in *NOAA/NWS/NCEP/MMAB Technical Note 316*, p. 194pp.

Torrence, C., and G. P. Compo (1998), A practical guide to wavelet analysis, *Bulletin of the American Meteorological Society*, *79*, 61–78.

Torrence, C., and P. J. Webster (1999), Interdecadal changes in the ENSO-Monsoon system, *Journal of Climate*, *12*, 2679–2690.

Van Enckevort, I. M. J., B. G. Ruessink, G. Coco, K. Susuki, I. L. Turner, N. G. Plant, and R. A. Holman (2004), Observations of nearshore crescentic sandbars, *Journal of Geophysical Research*, *109*, C06028, doi:10.1029/2003JC002214.

Wang, X. L., Y. Feng, and V. R. Swail (2012), North atlantic wave height trends as reconstructed from the 20th century reanalysis, *Geophysical Research Letters*, *39*(18), doi:10.1029/2012GL053381, l18705.

Wang, X. L., Y. Feng, and V. R. Swail (2014), Changes in global ocean wave heights as projected using multimodel cmip5 simulations, *Geophysical Research Letters*, *41*(3), 1026–1034, doi:10.1002/2013GL058650.

Yates, M. L., R. T. Guza, and W. C. O'Reilly (2009), Equilibrium shoreline response: Observations and modeling, *Journal of Geophysical Research*, *114*(C09014), doi:10.1029/2009JC005359.

Young, I. R., S. Zieger, and A. V. Babanin (2011), Global Trends in Wind Speed and Wave Height, *Science*, *332*(6028), doi:10.1126/science.1197219.

Zappa, G., L. C. Shaffrey, K. I. Hodges, P. G. Sansom, and D. B. Stephenson (2013), A multimodel assessment of future projections of north atlantic and european extratropical cyclones in the cmip5 climate models, *Journal of Climate*, *26*(16), 5846–5862, doi: 10.1175/JCLI-D-12-00573.1.

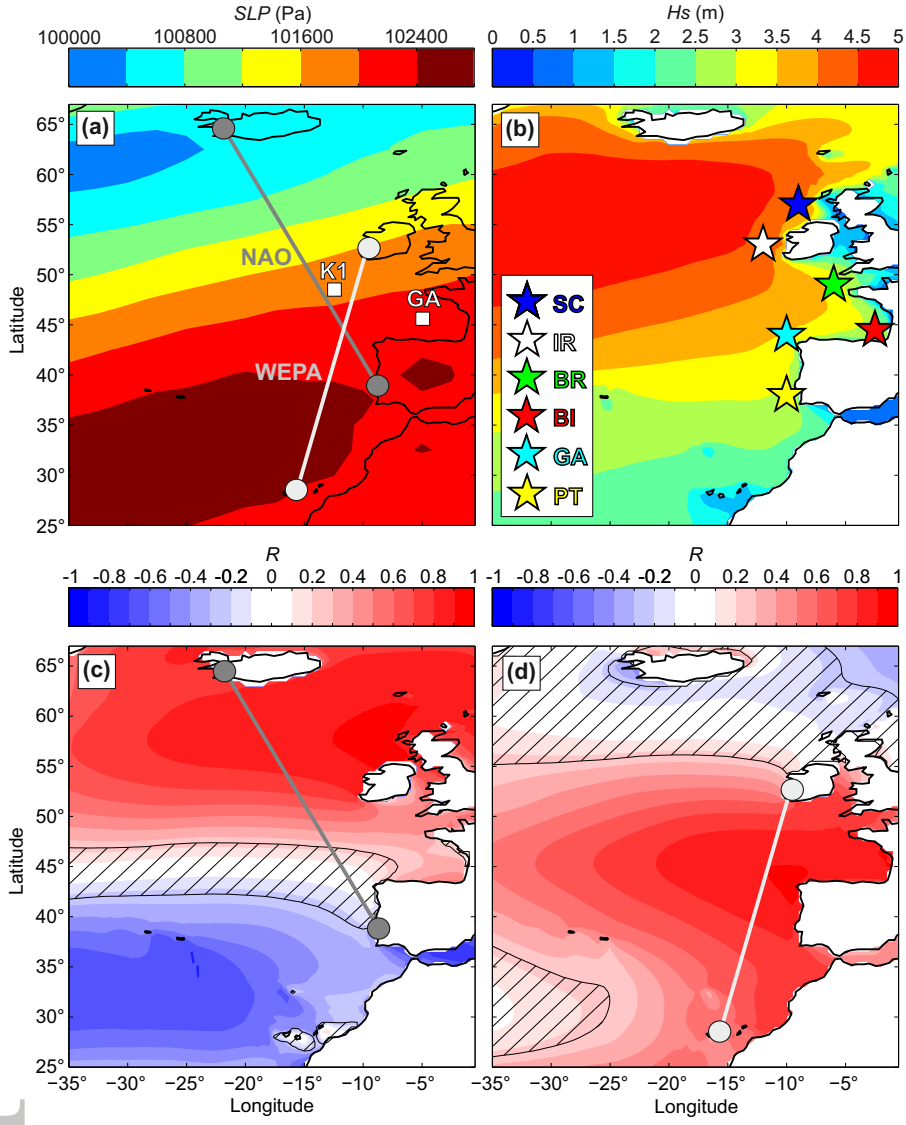

Figure 1. Top panels: winter-mean (DJFM, 1949-2017) (a) SLP and (b) Hs; bottom panels: spatial correlation of the winter-mean Hs against the winter(DJFM)-averaged (c) NAO and (d) WEPA indices. The NAO and WEPA indices defined as the normalized SLP difference measured between 2 stations are indicated by the dark and light grey circles in panels (a,c,d). The two white squares in (a) K1 and GA indicate the location of two relevant operated wave buoys used for validation. The 6 virtual wave buoys along the west coast of Europe are shown in panel (b), with SC: Scotland; IR: Ireland; BR: Brittany; BI: Biscay; GA: Galicia; PT: Portugal. The hatched zones are the areas where correlations are not significant at the 95% confidence level.

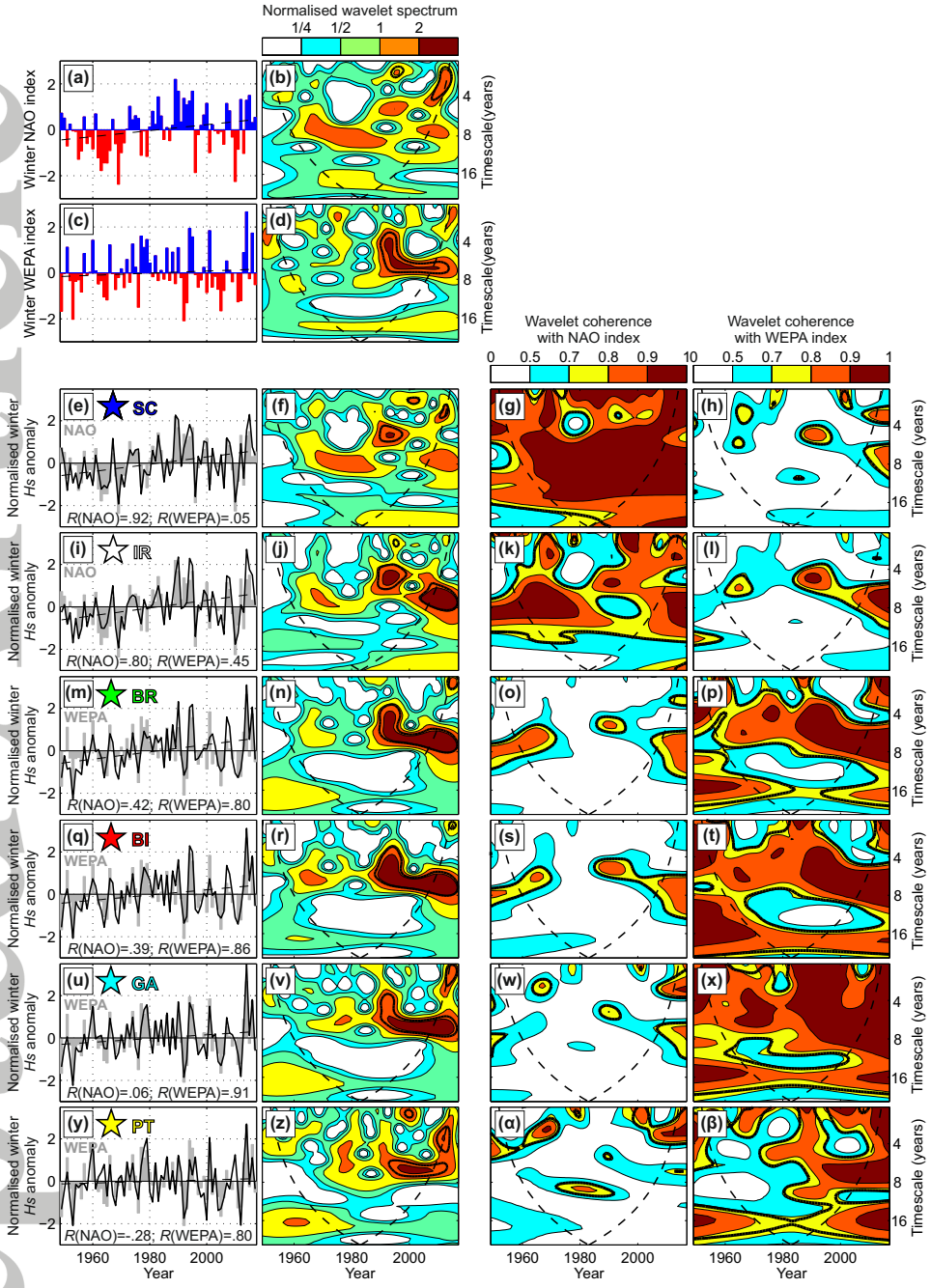

Figure 2. First column: time series of (a) NAO and (b) WEPA indices, with the 6 bottom panels showing, for the 6 virtual buoys, the time series of the normalized winter-mean Hs anomaly (black line) and its linear trend (dotted black line) superimposed onto the climate index (gray bars) with which the best correlation is found: (e,i): NAO; (m,q,u,y): WEPA. Second column: local wavelet spectrum normalized by the variance of the (b) NAO and (d) WEPA indices and, for the 6 bottom panels, of the normalized winter Hs anomaly. Third and fourth columns show the wavelet coherency-squared diagram normalized with the variance between the winter Hs at the 6 virtual buoys, and the NAO and WEPA indices, respectively. In all wavelet panels, the 5 % significance level against red noise is contoured in thick black, and the cone of influence is delimited by the dashed black line.

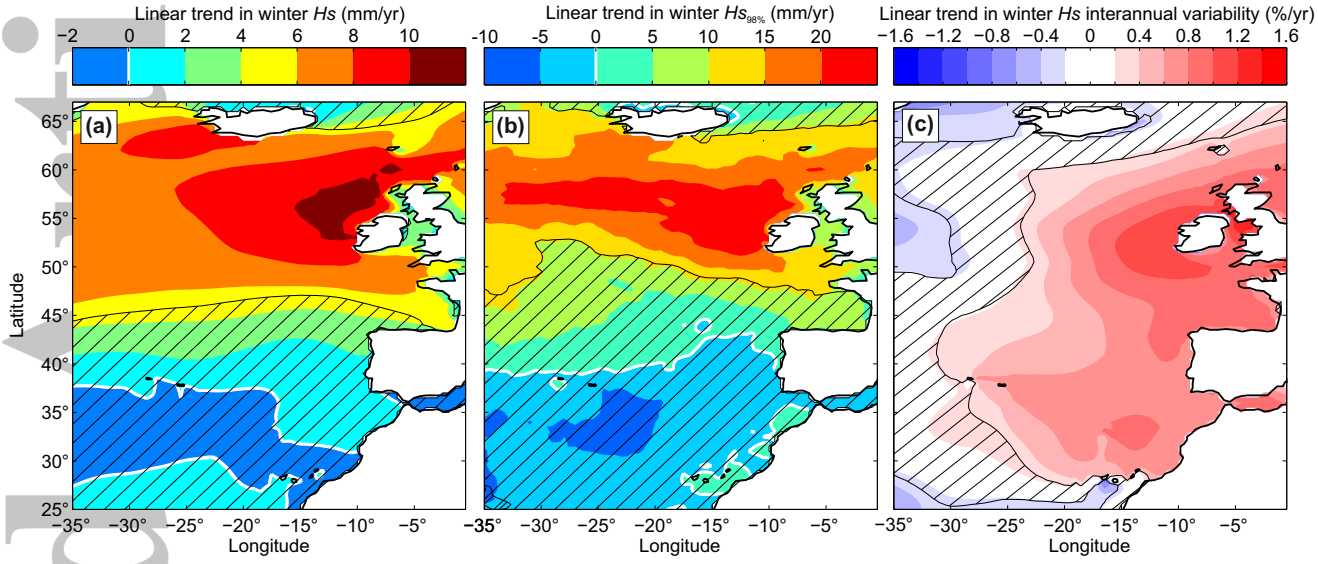

Figure 3. Linear trend of (a) winter-mean (1949-2017) Hs and (b) its 98% exceedance values $Hs_{98\%}$in mm/year, and of (c) winter-mean (1949-2017) Hs interannual variability in %/year. The hatched zones are areas where trends and correlations are not significant at the 95% confidence level.

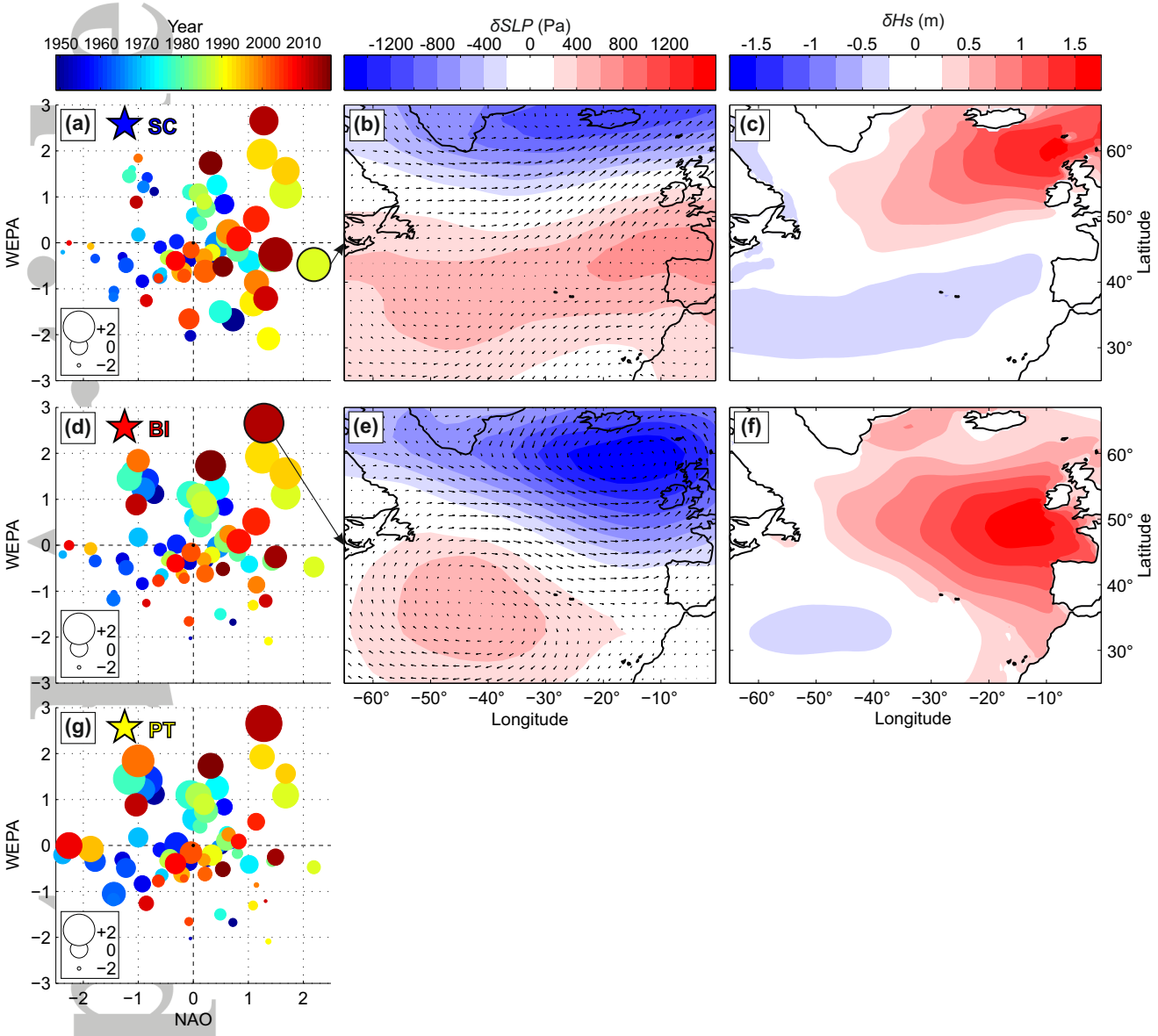

Figure 4. Left-hand panels: WEPA index versus NAO index for the 69 DJFM winters (1949-2017) with the winter year colored and the circle size proportional to the normalized winter-mean Hs anomaly at the buoys (a) SC: Scotland; (d) BI: Biscay and (g) PT: Portugal. The 4 right-hand panels show the atmospheric and wave height expression of the 2 winters with (b,c) the highest Hurrell-definition NAO index (1988/1989) and (e,f) the highest WEPA index (2013/2014) with (b,e) the winter-mean SLP anomaly with superimposed $\vec{u}_{10}$ field and (c,f) the winter-mean Hs anomaly.